Protein Science (1995), *4*:2605-2615. Cambridge University Press. Printed in the USA.

Structural and dynamic characterization of the urea denatured state of the immunoglobulin binding domain of streptococcal protein G by multidimensional heteronuclear NMR spectroscopy

M. KIRSTEN FRANK, G. MARIUS CLORE, AND ANGELA M. GRONENBORN

Laboratory of Chemical Physics, Building 5, National Institute of Diabetes and Digestive and Kidney Diseases, National Institutes of Health, Bethesda, Maryland 20892-0520

(RECEIVED August 28, 1995; ACCEPTED October 6, 1995)

Abstract

The structure and dynamics of the urea-denatured B1 immunoglobulin binding domain of streptococcal protein G (GB1) has been investigated by multidimensional heteronuclear NMR spectroscopy. Complete ^{1}H, ^{15}N, and ^{13}C assignments are obtained by means of sequential through-bond correlations. The nuclear Overhauser enhancement, chemical shift, and $^{3}J_{HN\alpha}$ coupling constant data provide no evidence for the existence of any significant population of residual native or nonnative ordered structure. ^{15}N relaxation measurements at 500 and 600 MHz, however, provide evidence for conformationally restricted motions in three regions of the polypeptide that correspond to the second β-hairpin, the N-terminus of the α-helix, and the middle of the α-helix in the native protein. The time scale of these motions is longer than the apparent overall correlation time (~3 ns) and could range from about 6 ns in the case of one model to between 4 μs and 2 ms in another; it is not possible to distinguish between these two cases with certainty because the dynamics are highly complex and hence the analysis of the time scale of this slower motion is highly model dependent. It is suggested that these three regions may correspond to nucleation sites for the folding of the GB1 domain. With the exception of the N- and C-termini, where end effects predominate, the amplitude of the subnanosecond motions, on the other hand, are fairly uniform and model independent, with an overall order parameter S^2 ranging from 0.4 to 0.5.

Keywords: B1 domain; backbone dynamics; ^{15}N relaxation; protein G; structure; unfolded state

The two-state model of protein unfolding in chemical denaturants is commonly used to analyze the stability of proteins. In this model, there is an unfolded state and a native state and the relative populations of these states are changed by the addition of the chemical denaturant. The energetics of this transition can be related to structural features of the native state, although, strictly speaking, the energetics depend on the difference in structure between the two states (Dobson, 1992; Shortle, 1993). It is possible that chemically denatured proteins have residual structure, thereby affecting the kinetics and thermodynamics of the transition from the unfolded to the folded state (Shortle & Abeygunawardana, 1993). If residual structure is a general feature of chemically denatured proteins, the two-state model would need to be modified to relate residual structure in the unfolded state to the energetics and kinetics of the folding reaction.

A series of recent NMR studies on the chemically denatured state of two proteins, 434 repressor (Neri et al., 1992a, 1992b, 1992c) and FK506-binding protein (Logan et al., 1993, 1994), have indicated the presence of residual structure, including, in the latter example, some secondary structure. Residual structure has also been found in the acid-denatured state of barnase (Arcus et al., 1994), the acid-denatured molten globule states of human ubiquitin (Stockman et al., 1993) and α-lactalbumin (Alexandrescu et al., 1993), a recombinant model of the reduced unfolded state of bovine pancreatic trypsin inhibitor (Lumb & Kim, 1994), a deletion mutant of staphylococcal nuclease (Alex-

Reprint requests to: G.M. Clore or A.M. Gronenborn, Laboratory of Chemical Physics, Building 5, National Institute of Diabetes and Digestive and Kidney Diseases, National Institutes of Health, Bethesda, MD 20892-0520; e-mail: clore@vger.niddk.nih.gov or gronenborn@vger.niddk.nih.gov.

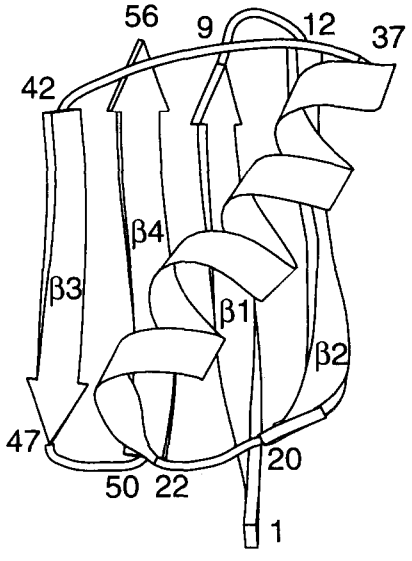

Fig. 1. Schematic ribbon diagram of the folded GB1 domain. The figure was generated with the program MOLSCRIPT (Kraulis, 1991) and the coordinates are taken from Gronenborn et al. (1991).

andrescu et al., 1994; Alexandrescu & Shortle, 1994), and the denatured form of a destabilizing mutant of staphylococcal nuclease (Shortle & Abeygunawardana, 1993). To date the dynamic behavior of unfolded or partially unfolded states has only been characterized to a very limited extent (Alexandrescu & Shortle, 1994; Farrow et al., 1995)

The B1 immunoglobulin binding domain of streptococcal protein G (GB1) can be described as a prototypic polypeptide for the purposes of studying protein folding (Kuszewski et al., 1994). In particular, it is a small 56-residue domain that is highly thermostable and contains no disulfide bridges, prolines, or prosthetic groups that could result in structural misorganization during the folding process. Its structure has been determined at high resolution by NMR (Gronenborn et al., 1991) and crystallography (Achari et al., 1992; Gallagher et al., 1994), and the dynamics of the folded state have been analyzed (Barchi et al., 1994). In the folded state, the GB1 domain is highly compact, with 95% of the residues participating in regular secondary structure. The GB1 domain comprises a four-stranded β-sheet arranged in a -1, $+3$x, -1 topology on top of which lies an α-helix (Fig. 1). The refolding kinetics from a pH denatured state have been studied by stopped-flow absorption spectroscopy (Alexander et al., 1992) and from the guanidinium chloride denatured state by quenched-flow deuterium-hydrogen exchange and stopped-flow fluorescence (Kuszewski et al., 1994). The latter study suggested that collapse to a semi-compact state exhibiting partial order and characterized by ND-NH exchange protection factors up to 10-fold higher than that expected for a random coil, occurs in less than 1 ms, followed by the formation of the fully native state in a single rapid concerted step with a half-life of about 5 ms (Kuszewski et al., 1994). No structural information, however, was available on the initial guanidinium chloride unfolded state of GB1. Therefore, there exists the distinct possibility that the semi-compact state inferred from the quenched-flow D-H exchange study represents the initial unfolded state of GB1.

Peptide fragments of GB1 have been studied in isolation in water and trifluoroethanol (Blanco et al., 1994a, 1994b), and it has been shown that a peptide comprising the β3–β4 turn exhibits a significant population of native conformer in water. A peptide comprising the β1–β2 turn, however, shows no evidence of residual structure in the absence of trifluoroethanol. Interestingly, the β3–β4 turn displays the highest ND-NH exchange protection factors in the collapsed state observed by Kuszewski et al. (1994) and is therefore a good candidate for having residual structure in the unfolded state.

In the present paper, we have set out to characterize the structural and dynamic properties of the urea-unfolded state of the GB1 domain using multidimensional heteronuclear NMR spectroscopy. Neither the ^{1}H, ^{15}N, and ^{13}C chemical shifts, nor the observed ^{1}H-^{1}H NOEs provide any firm evidence for the presence of residual structure in the urea-unfolded state of GB1. ^{15}N-relaxation measurements, however, suggest that the region comprising the β3–β4 turn in the native state is conformationally more restricted in the unfolded state than the rest of the protein.

Results and discussion

Equilibrium unfolding of the GB1 domain in urea

In order to establish optimal conditions for studying the unfolded state of the GB1 domain by NMR, we first established the equilibrium unfolding curve as a function of urea. The results at pH 2 and 25 °C are shown in Figure 2. The unfolding transition is clearly two-state, with a transition point occurring at about 3.7 M urea, and the GB1 domain is completely unfolded above 6 M urea. At higher pH values, 100% occupancy of the unfolded state could not be obtained even at saturating concentrations of urea. Analysis of the data as described by Pace et al. (1989) yields a free energy of unfolding in water, $\Delta G(H_2O)$, of 4.1 kcal·mol^{-1} at pH 2. Thus, the GB1 domain is approximately 15% less stable at pH 2 than at pH 4, where

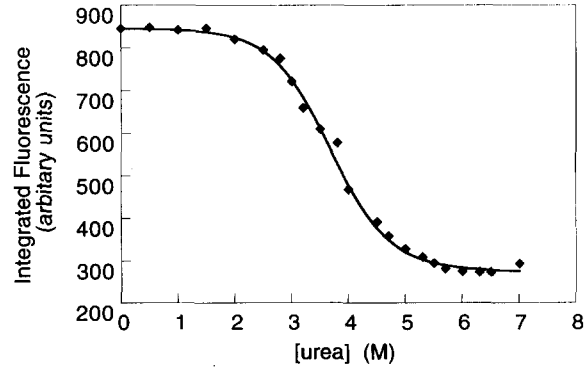

Fig. 2. Equilibrium unfolding of the GB1 domain at pH 2 and 25 °C in urea as monitored by the fluorescence of the single tryptophan residue at position 43. (Fluorescence excitation was carried out at 295 nm and the emission was integrated from 305 to 450 nm.) The experimental points are represented as solid cicles, and the line represents the nonlinear least-squares best fit to a two-state model (Pace et al., 1989) with a $\Delta G(H_2O)$ value of 4.10 kcal·mol^{-1} and a transition point of 3.67 M urea.

$\Delta G(H_2O)$ has a value of 4.8 kcal·mol^{-1}, as determined from a guanidinium chloride unfolding study (Kuszewski et al., 1994). With these data in hand, we proceeded to characterize the unfolded state of GB1 by NMR at pH 2 in 7.4 M urea. We note that we did not carry out this study at pH 4 using guanidinium chloride as a denaturant because, in contrast to urea, guanidinium chloride is ionic and the ionic strength required (~4.5 M) reduces the quality factor (Q) of the NMR probe significantly, thereby dramatically reducing the signal-to-noise ratio.

^1H, ^{13}C and ^{15}N assignments of unfolded GB1

The ^1H-^{15}N HSQC correlation spectrum of denatured GB1 in 7.4 M urea, pH 2, and 25 °C is shown in Figure 3. Cross peaks for all 55 backbone amide groups can be identified. As is evident, the chemical shifts of the backbone amide proton resonances are clustered in a narrow 0.7-ppm window between 8.0 and 8.7 ppm, typical of a denatured protein. In addition, cross peaks for the side-chain amides of three out of four carboxyamide groups (three asparagines and one glutamine, between 7 and 7.7 ppm and between 111.5 and 112.5 ppm for ^1H and ^{15}N, respectively), the Nϵ1H of the single Trp ring (10.1 ppm and 129.0 ppm for ^1H and ^{15}N, respectively), and the NζH^{3+} group of lysine residues (7.68 ppm and 32.7 ppm for ^1H and ^{15}N, respectively) are also visible in the ^1H-^{15}N HSQC spectrum. ^1H, ^{13}C, and ^{15}N chemical shift assignments (Table 1) were obtained using three-dimensional heteronuclear NMR spectroscopy to trace through-bond heteronuclear correlations along the backbone and side chains. For this purpose, the following 3D experiments were recorded: ^{15}N-separated HOHAHA, HNHA, CBCANH, HBHA(CBCA)NH, CBCA(CO)NH, HBHA(CO)NH, C(CO)NH, and H(CCO)NH experiments in H_2O, and ^{13}C-separated HCCH-TOCSY and HCCH-COSY and ^{13}C-^{13}C-^1H AMNESIA experiments in D_2O (see Bax & Grzesiek [1993], Clore & Gronenborn [1991, 1994] for reviews and citations to original references and Wang et al. [1994] and Grzesiek & Bax [1995] for the HBHA(CBCA)NH and AMNESIA experiments, respectively). Examples of strips taken from the CBCANH, HBHA(CBCA)NH, C(CO)NH, and H(CCO)NH experiments that demonstrate C$\alpha(i-1, i)$/C$\beta(i, i-1)$-N(i)-NH(i), H$\alpha(i-1, i)$/H$\beta(i-1, i)$-N(i)-NH(i), C($i-1$)-N(i)-NH(i) and H($i-1$)-N(i)-NH(i) connectivities, respectively, are shown in Figure 4A, B, C, and D. A summary of the deviations from random coil of the $^{13}C\alpha$, $^{13}C\beta$, $^1H\alpha$, and $^1H\beta$ shifts as a function of residue is provided in Figure 5.

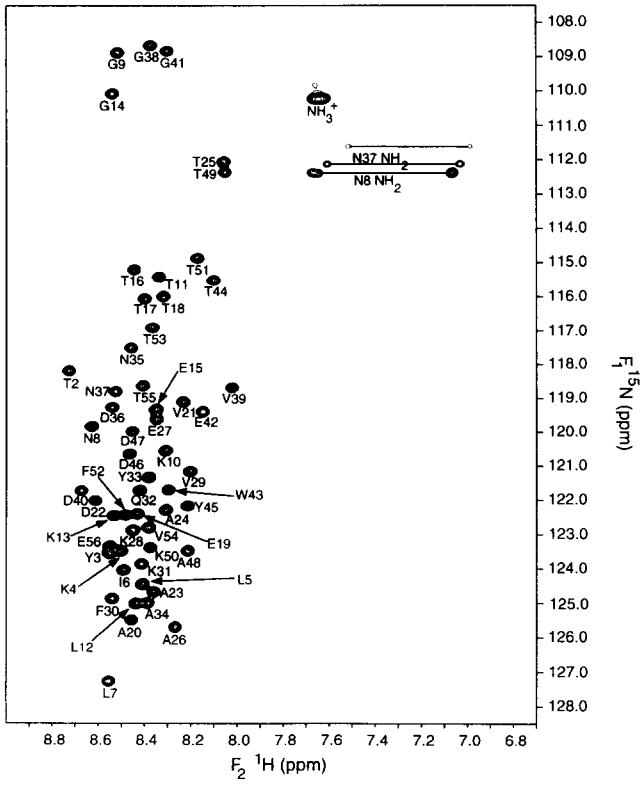

Fig. 3. ^1H-^{15}N HSQC spectrum of urea-unfolded GB1 at 7.4 M urea, pH 2, 25 °C. Note that the NH_3^+ peak arising from the side chain of the Lys residues is folded in the ^{15}N dimension from 32.7 ppm, and that the indole NϵH group of the single Trp residue, which resonates at 10.1 ppm in ^1H and 129.0 ppm in ^{15}N, is not shown.

The bulk of the ^{15}N shifts for the backbone amides are clustered between 117.7 and 127.4 ppm. The ^{15}N shifts of the Thr and Gly residues, however, are distinct from the rest, resonating between 112.3 and 118.8 ppm, and between 109.0 and 110.2 ppm, respectively. There are nine pairs of identical dipeptides within the sequence (Table 2). In general, the ^{15}N shifts for these pairs tend to be similar. There is one exception, namely the Thr-Tyr pair involving Tyr 3 and Tyr 45. In this particular case, Tyr 3 is the third residue of the polypeptide and hence its amide nitrogen will be substantially influenced by the charge on the free amino terminus.

It is interesting to note that the ^{15}N shifts of the backbone amides of Thr 25 and Thr 49 are upfield shifted by 3–4 ppm relative to those of the other Thr residues in the sequence. We attribute this phenomenon to the presence of a preceding Ala residue. Indeed, similar upfield ^{15}N shifts of the backbone amide of Thr have been observed in the only three other reported examples of an Ala-Thr dipeptide sequence within an unfolded protein (Shortle & Abeygunawardana, 1993; Logan et al., 1994; Zhang et al., 1994). This effect may arise from a specific contribution of the methyl group of the preceding Ala residue on the ^{15}N shielding of the backbone amide of the following Thr residue (Le & Oldfield, 1994).

The ^{13}C shifts of urea-unfolded GB1 are close to those in small model polypeptides that are thought to mimic random coil behavior (Spera & Bax, 1991). In comparing our ^{13}C shifts to model peptide data, it was important to correct the random coil values for the Asp and Glu residues to take into account the fact that these residues are protonated under our pH conditions (namely pH 2). To this end, we used the data from Richarz and Wüthrich (1978) to estimate random coil values for the protonated forms of the Asp and Glu residues, assuming a constant difference between the Richarz and Wüthrich (1978) data on the one hand, and the Spera and Bax (1991) and Wishart et al. (1995) data on the other. The RMS differences between the $^{13}C\alpha$ and $^{13}C\beta$ shifts for urea-unfolded protein G and the data of Wishart et al. (1995), derived from model peptide with the sequence Gly-Gly-X-Ala-Gly-Gly, are 0.29 and 0.24 ppm, respectively. The corresponding numbers versus the random coil values of Spera and Bax (1991) are slightly larger, 0.38 and 0.76 ppm, respectively. A similar comparison of the ^1H shifts of the unfolded GB1 with that of the peptide random coil shifts

Table 1. *^{1}H, ^{13}C, and ^{15}N assignments of the unfolded GB1 domain in 7.4 M urea, pH 2, 25 °C*[a]

Residue	N	Cα	Cβ	Others
Met 1		55.2 (4.29)	32.9 (2.20, 2.20)	Cγ 31.2 (2.63,2.53)
Thr 2	118.3 (8.72)	61.8 (4.51)	70.3 (4.20)	Cγ 21.9 (1.30)
Tyr 3	123.7 (8.54)	57.9 (4.71)	39.4 (3.13, 2.98)	Cδ 133.4 (7.25); Cε 118.3 (6.92)
Lys 4	123.6 (8.49)	56.2 (4.40)	33.6 (1.83,1.79)	Cγ 25.1 (1.50, 1.42); Cδ 29.3 (1.77, 1.77); Cε 42.3 (3.06, 2.89)
Leu 5	124.5 (8.40)	55.2 (4.44)	42.8 (1.66,1.66)	Cγ 27.4 (1.67); Cδ 24.7 (1.04), 24.1 (1.01)
Ile 6	124.2 (8.48)	60.9 (4.27)	38.6 (1.93)	Cγ 27.4 (1.59,1.25); Cγm 17.5 (0.97); Cδ 12.7 (0.98)
Leu 7	127.4 (8.55)	54.9 (4.53)	42.6 (1.73,1.67)	Cγ 27.1 (1.68); Cδ 25.1 (1.04), 23.5 (0.98)
Asn 8	120.0 (8.62)	53.4 (4.82)	39.1 (2.95,2.93)	Nδ 112.4 (7.67, 7.08)
Gly 9	109.0 (8.51)	45.6 (4.14, 4.07)		
Lys 10	120.7 (8.30)	56.5 (4.52)	33.5 (1.95, 1.87)	Cγ 25.1 (1.56, 1.54); Cδ 29.2 (1.96, 1.80); Cε 42.1 (3.10, 3.02)
Thr 11	115.6 (8.33)	62.0 (4.47)	70.1 (4.31)	Cγ 22.0 (1.32)
Leu 12	125.2 (8.44)	55.2 (4.48)	42.6 (1.71, 1.66)	Cγ 27.3 (1.71); Cδ 25.0 (1.00), 23.8 (1.00)
Lys 13	122.6 (8.53)	56.8 (4.40)	33.4 (1.92, 1.86)	Cγ 25.0 (1.58, 1.51); Cδ 29.0 (1.95, 1.82); Cε 42.4 (3.08)
Gly 14	110.2 (8.54)	45.4 (4.08, 4.03)		
Glu 15	119.7 (8.34)	55.9 (4.59)	29.4 (2.24, 2.11)	Cγ 33.0 (2.60, 2.60)
Thr 16	115.4 (8.44)	62.0 (4.58)	70.1 (4.38)	Cγ 21.8 (1.34)
Thr 17	116.2 (8.39)	62.0 (4.57)	70.1 (4.38)	Cγ 21.8 (1.33)
Thr 18	116.1 (8.31)	62.1 (4.46)	70.0 (4.34)	Cγ 21.8 (1.33)
Glu 19	122.6 (8.42)	55.9 (4.47)	29.1 (2.20, 2.09)	Cγ 32.9 (2.74, 2.60)
Ala 20	125.6 (8.45)	52.8 (4.45)	19.2 (1.48)	
Val 21	119.3 (8.23)	62.7 (4.16)	33.0 (2.16)	Cγ 21.1 (1.05)
Asp 22	122.2 (8.61)	52.9 (4.82)	38.2 (3.09, 2.96)	
Ala 23	124.8 (8.35)	53.0 (4.38)	19.4 (1.50)	
Ala 24	122.4 (8.30)	53.1 (4.42)	19.2 (1.54)	
Thr 25	112.2 (8.06)	61.9 (4.37)	69.9 (4.31)	Cγ 21.9 (1.29)
Ala 26	125.9 (8.26)	52.8 (4.42)	19.4 (1.50)	
Glu 27	119.5 (8.35)	56.0 (4.42)	29.0 (2.22, 2.11)	Cγ 32.9 (2.57, 2.57)
Lys 28	123.0 (8.45)	56.5 (4.40)	33.3 (1.90, 1.80)	Cγ 25.2 (1.50, 1.43); Cδ 29.3 (1.95, 1.87); Cε 42.4 (3.08, 3.06)
Val 29	121.3 (8.20)	62.2 (4.19)	33.3 (2.06)	Cγ 21.0 (0.98), 21.0 (0.97)
Phe 30	125.0 (8.53)	57.7 (4.74)	40.0 (3.18, 3.07)	Cδ 132.2 (7.34); Cε 131.4 (7.42)
Lys 31	124.0 (8.41)	56.2 (4.33)	33.5 (1.90, 1.74)	Cγ 25.0 (1.44, 1.38); Cδ 29.2 (1.77, 1.74); Cε 42.2 (3.06, 3.03)
Gln 32	121.9 (8.42)	56.1 (4.32)	29.8 (2.07, 1.99)	Cγ 33.9 (2.34, 2.34)
Tyr 33	121.5 (8.38)	57.8 (4.67)	39.1 (3.19, 2.98)	Cδ 133.4 (7.23); Cε 118.3 (6.92)
Ala 34	125.1 (8.38)	52.6 (4.39)	19.6 (1.45)	
Asn 35	117.7 (8.45)	53.3 (4.78)	39.0 (2.94, 2.86)	
Asp 36	119.4 (8.53)	53.1 (4.84)	38.1 (3.05, 2.96)	
Asn 37	118.9 (8.52)	53.7 (4.82)	39.0 (2.92, 2.87)	Nδ 112.1 (7.61, 7.03)
Gly 38	108.8 (8.37)	45.6 (4.03, 3.94)		
Val 39	118.8 (8.02)	62.6 (4.21)	32.8 (2.17)	Cγ 21.3 (1.01), 20.7 (1.01)
Asp 40	121.9 (8.67)	53.3 (4.83)	38.2 (3.07, 2.95)	
Gly 41	109.0 (8.30)	45.6 (3.97, 3.97)		
Glu 42	119.5 (8.14)	56.0 (4.40)	29.0 (2.06, 2.01)	Cγ 32.8 (2.43, 2.39)
Trp 43	121.8 (8.29)	57.3 (4.85)	29.9 (3.30, 3.27)	Cζ2 135.4 (7.56); Cε3 121.0 (7.68); Cη2 124.8 (7.31); Cδ1 127.1 (7.26); Cζ3 122.2 (7.19); Nε1 129.0 (10.09)
Thr 44	115.7 (8.10)	61.8 (4.39)	70.3 (4.17)	Cγ 21.5 (1.16)
Tyr 45	122.3 (8.21)	58.3 (4.55)	38.9 (3.09, 2.98)	Cδ 133.4 (7.15); Cε 118.3 (6.91)
Asp 46	120.8 (8.46)	52.9 (4.77)	38.2 (3.04, 2.86)	
Asp 47	120.1 (8.45)	53.2 (4.74)	38.2 (3.01, 2.91)	
Ala 48	123.6 (8.21)	53.2 (4.44)	19.4 (1.52)	
Thr 49	112.3 (8.05)	62.1 (4.41)	70.0 (4.31)	Cγ 21.9 (1.33)
Lys 50	123.5 (8.37)	56.5 (4.42)	33.2 (1.88, 1.85)	Cγ 25.0 (1.51, 1.46); Cδ 29.8 (1.80, 1.77); Cε –(3.06, 3.06)
Thr 51	115.0 (8.17)	61.6 (4.44)	70.4 (4.22)	Cγ 21.8 (1.25)
Phe 52	122.6 (8.48)	57.8 (4.86)	40.2 (3.23, 3.10)	Cδ 132.2 (7.34); Cε 131.4 (7.42); Cζ –(7.55)
Thr 53	117.1 (8.36)	61.8 (4.50)	70.4 (4.22)	Cγ 21.8 (1.28)
Val 54	123.0 (8.37)	62.3 (4.30)	33.2 (2.16)	Cγ 21.3 (1.04)
Thr 55	118.8 (8.40)	62.1 (4.46)	70.1 (4.25)	Cγ 21.9 (1.32)
Glu 56	123.5 (8.54)	55.0 (4.55)	28.8 (2.31, 2.10)	Cγ 32.7 (2.60, 2.60)

[a] In each column, the ^{15}N and ^{13}C shifts are listed first and the ^{1}H shifts are given in parentheses. ^{1}H and ^{13}C shifts are reported relative to 3-(trimethylsilyl)propanoic-d_4 acid and ^{15}N shifts relative to liquid ammonia.

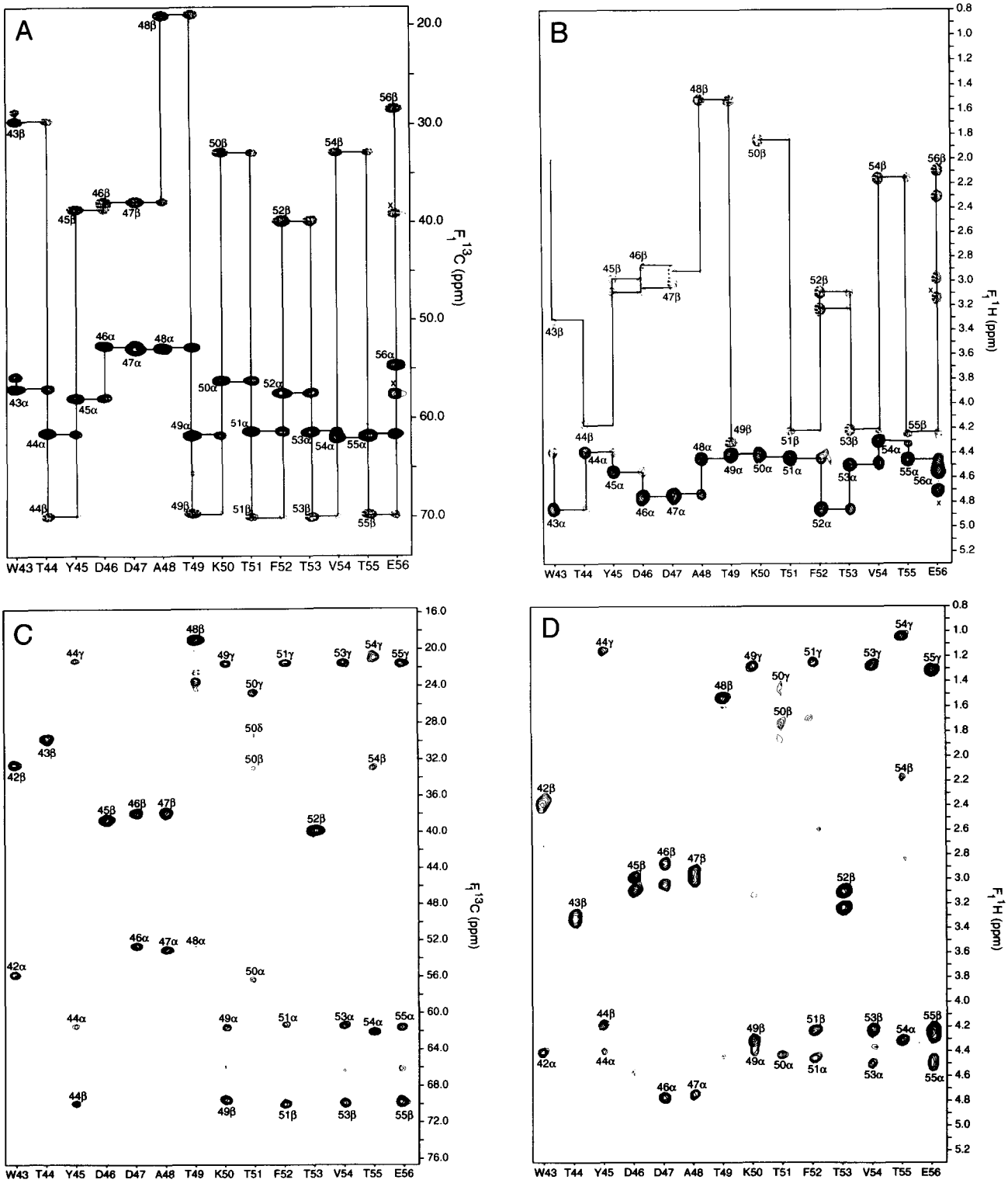

Fig. 4. Strips taken from the **(A)** 3D CBCANH, **(B)** HBHA(CBCA)NH, **(C)** C(CO)NH, and **(D)** H(CCO)NH experiments illustrating the through-bond directed sequential assignment of unfolded GB1. The peaks marked with an x in the strip for Glu 56 arise from Tyr 3 and have their maximum intensity in a neighboring plane of the 3D spectra.

obtained by Bundi and Wüthrich (1979), Merutka et al. (1995), and Wishart et al. (1995) yielded an RMS difference of 0.12, 0.13, and 0.13 ppm, respectively, for the Hα protons, 0.08, 0.07, and 0.08 ppm, respectively, for the Hβ protons. A summary of the average $^{13}C\alpha$, $^{13}C\beta$, $^{1}H\alpha$, and $^{1}H\beta$ shifts for each residue type in unfolded GB1 is presented in Table 3. These shifts may be more indicative of random coil shifts in full-length proteins than the shifts derived from short model peptides.

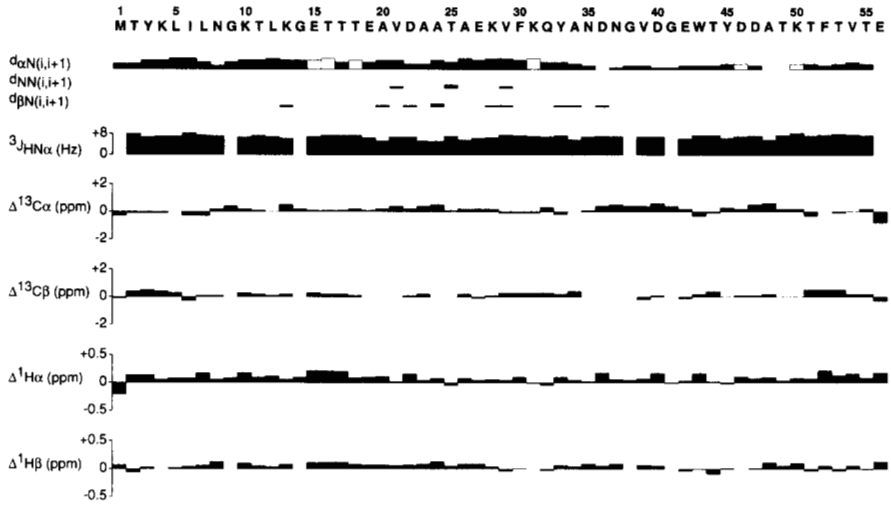

Fig. 5. Summary of the backbone NOEs, $^3HN\alpha$ couplings constants, and deviations from random coil shifts for the $^{13}C\alpha$, $^{13}C\beta$, $^1H\alpha$, and $^1H\beta$ resonances of unfolded GB1. Random coil values are taken from Wishart et al. (1995). Open boxes for the $d_{\alpha N(i+1)}$ connectivities represent those NOEs where overlap precluded the distinction between intraresidue and sequential interresidue NOEs.

Analysis of NOE and coupling constant data for unfolded GB1

To assess the presence of any residual structure, $^3J_{HN\alpha}$ coupling constants were obtained from a 3D HNHA (Vuister & Bax, 1993) experiment, and 3D ^{15}N and ^{13}C-separated NOE spectra (Marion et al., 1989; Ikura et al., 1990) were recorded.

The $^3J_{HN\alpha}$ coupling constants ranged from 5 to 8 Hz (Fig. 5) with an average value of 6.9 ± 0.7 Hz and provided no evidence for the presence of any α-helix, β-sheet, or β-turns. Likewise, the NOE data yielded no evidence for any nonsequential NOEs indicative of the presence of residual structure. A summary of the $^3J_{HN\alpha}$ coupling constants and the NOEs involving the NH, CαH and CβH protons is provided in Figure 5, and examples of strips taken from the 3D ^{15}N-separated NOE spectrum illustrating the NOE connectivities extending from residues 43 to 56 is shown in Figure 6. In general, sequential CαH(i)-NH($i+1$) NOEs are apparent for most of the polypeptide chain. Only three weak NH(i)-NH($i+1$) NOEs, however, are observed (between Thr 25 and Ala 26, Val 29 and Thr 30, Val 39 and Asp 40). A few other sequential NOEs involving side chains are also seen: namely from Ile 6(Cγ_mH$_3$) to Leu 7(CαH), from Val 21(CγH$_3$) to Ala 20(CαH), from Lys 28(CγH) to Val 29(CαH), and from Val 39(CγH$_3$) to Gly 38(CαH) and Asp 40(CαH). A sizeable set of NOEs was observed between Tyr 33 and Ala 34, in particular from Tyr 33(CβH) to Ala 34(CαH), from Tyr 33(CδH) to Ala 34(CαH) and Ala 34(CβH), and from Tyr 33(CϵH) to Ala 34(CβH). This is in agreement with observations that aromatic side chains in small peptides interact with the two residues immediately C-terminal to the aromatic residue (Merutka et al., 1995; Wishart et al., 1995). In a similar vein, a weak NOE was observed between Tyr 3(CϵH) and Leu 5(Cδ_bH$_3$).

A small 16-residue peptide corresponding to the second β-hairpin in GB1 (residues 41–56; Fig. 1) has been shown by NMR to

Table 2. *Pairs of identical dipeptides present in the sequence of the GB1 domain*

Dipeptide	Residue numbers
Thr-Tyr	2–3, 44–45
Asn-Gly	8–9, 37–38
Val-Asp	21–22, 39–40
Thr-Thr	16–17, 17–18
Ala-Thr	24–25, 48–49
Gly-Glu	14–15, 41–42
Lys-Thr	10–11, 50–51
Thr-Glu	18–19, 55–56
Asp-Ala	22–23, 47–48

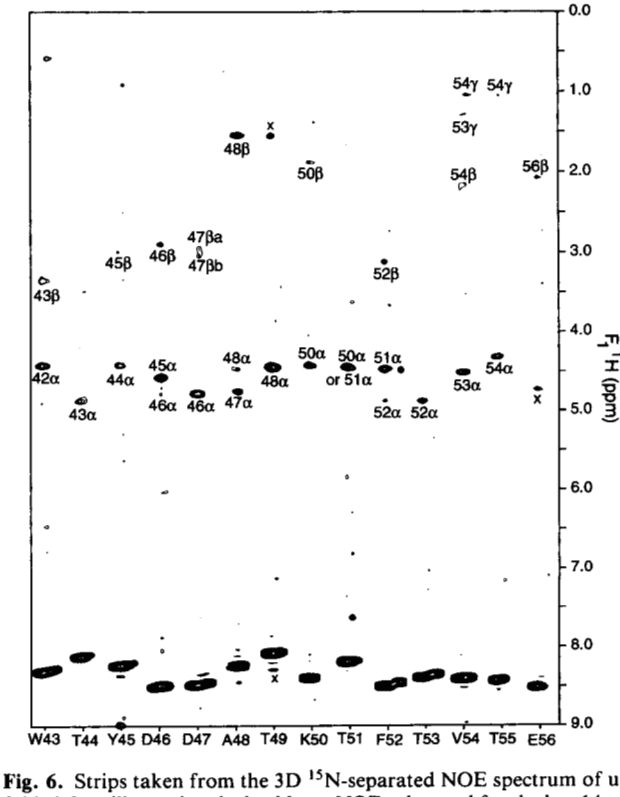

Fig. 6. Strips taken from the 3D ^{15}N-separated NOE spectrum of unfolded GB1 illustrating the backbone NOEs observed for the last 14 residues of the polypeptide, which includes the residues that form the second β-hairpin in native GB1.

Table 3. *Average values of ^{15}N, $^{13}C\alpha$, $^{13}C\beta$, $^{1}H\alpha$, and $^{1}H\beta$ chemical shifts for the various residues in the urea-unfolded GB1 domain*[a]

Residue[b]	^{15}N	$^{13}C\alpha$	$^{13}C\beta$	$^{1}H\alpha$	$^{1}H\beta$
Ala (6)	124.6 ± 1.3	52.9 ± 0.2	19.4 ± 0.2	4.41 ± 0.04	1.50 ± 0.03
Asn (3)	118.9 ± 1.2	53.5 ± 0.2	39.0 ± 0.1	4.81 ± 0.02	2.94 ± 0.01, 2.89 ± 0.03
Asp (5)	120.9 ± 1.2	53.1 ± 0.2	38.2 ± 0.04	4.80 ± 0.04	3.06 ± 0.03, 2.93 ± 0.04
Gln (1)	121.9	56.1	29.8	4.32	2.02, 2.07
Gly (4)	109.3 ± 0.6	45.6 ± 0.1		4.06 ± 0.06, 4.00 ± 0.05	
Glu (5)	120.9 ± 1.9	55.8 ± 0.4	29.1 ± 0.2	4.49 ± 0.07	2.21 ± 0.08, 2.08 ± 0.04
Ile (1)	124.2	60.9	38.6	4.27	1.93
Leu (3)	125.7 ± 1.5	55.1 ± 0.2	42.7 ± 0.1	4.48 ± 0.04	1.70 ± 0.03, 1.66 ± 0.004
Lys (6)	122.9 ± 1.2	56.5 ± 0.2	33.4 ± 0.2	4.41 ± 0.06	1.91 ± 0.04, 1.82 ± 0.05
Met (1)	–	55.2	32.9	4.29	2.20, 2.20
Phe (2)	123.8 ± 1.7	57.8 ± 0.1	40.1 ± 0.1	4.80 ± 0.06	3.20 ± 0.02, 3.08 ± 0.01
Thr (11)	115.7 ± 2.1	62.0 ± 0.2	70.2 ± 0.2	4.47 ± 0.07	4.28 ± 0.07
Trp (1)	121.8	57.3	29.9	4.86	3.30
Tyr (3)	122.5 ± 1.1	58.0 ± 0.3	39.1 ± 0.3	4.65 ± 0.07	3.14 ± 0.04, 2.98 ± 0.002
Val (4)	120.6 ± 1.9	62.5 ± 0.2	33.1 ± 0.2	4.22 ± 0.05	2.14 ± 0.04

[a] ^{1}H and ^{13}C shifts are referenced relative to 3-(trimethylsilyl)propanoic-d_4 acid; ^{15}N shifts relative to liquid ammonia.
[b] Number of occurences in parentheses.

be monomeric and to adopt at pH 6.3 and 5 °C a population containing approximately 40% and 20% of the native-like β-hairpin structure in pure water (Blanco et al., 1994b) and 6 M urea (Blanco & Serrano, 1995), respectively. We see no evidence that this turn is populated in urea-unfolded GB1. Specifically, the strong sequential NH(i)-NH(i + 1) NOEs between residues 47–51 that identify the turn are not observed in urea-unfolded GB1. Similarly, the 0.3 ppm difference between the CαH shifts of Asp 46 and Asp 47 that is observed in the isolated peptide in water and 6 M urea at pH 6.3 and 5 °C, is not seen in the unfolded GB1 domain in 7.4 M urea, pH 2, and 25 °C (where the difference in ^{1}H chemical shift is only 0.03 ppm).

Dynamics of urea-unfolded GB1

Although the NOE and coupling constant data provide no evidence for any residual structure, it is possible that transient medium- or long-range structures may be manifested in the backbone dynamics of unfolded GB1. To this end, we carried out ^{15}N relaxation measurements at 500 and 600 MHz on unfolded GB1. The resulting ^{15}N T_1, T_2, and ^{1}H-^{15}N NOE data are summarized in Figure 7. The T_1, T_2, and NOE values appear to be quite uniform with two exceptions. First, there are clear-cut end effects at the N- (residues 2–4) and C- (residues 53–56) termini manifested by longer T_1 and T_2 values and large negative NOE values. Excluding these residues, the average T_1, T_2, and NOE values (for residues 5–52) are 592 ± 34 ms, 330 ± 47 ms, and −0.04 ± 0.13, respectively. Second, the T_1 values are systematically shortened between residues 42–48, and the T_2 values at both 500 and 600 MHz are systematically shortened between residues 21–22, 28–33, and 43–51. In general, the values of the relaxation parameters at 500 and 600 MHz follow each other closely. There are a few exceptions, in particular at the N- and C-termini, presumably as a result of end effects complicating the motion. Also, there are a few additional regions where the NOE values at 500 and 600 MHz appear to differ quite sig-

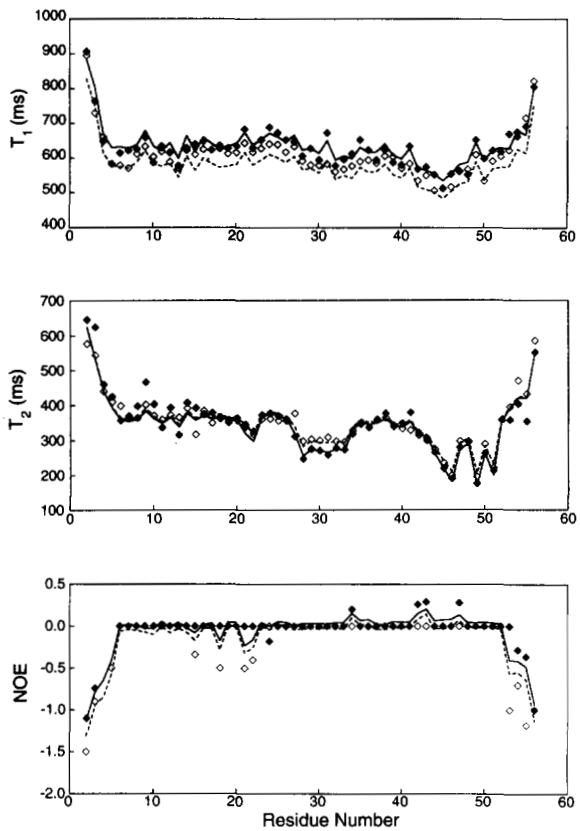

Fig. 7. Summary of the ^{15}N T_1, T_2, and NOE relaxation data for the unfolded GB1 domain. Data collected at 500 and 600 MHz are represented as open and closed diamonds, respectively. Dashed and solid lines represent the global best fit to the data at 500 and 600 MHz, respectively, using Model 2 (cf. the spectral density function represented by Equation 2). Fitting errors in the T_1 and T_2 values are generally ≤2% and are smaller than the symbols, and errors in the measured NOE values are ±0.1–0.15.

nificantly, with the values at one frequency being zero, and at the other, either negative (e.g., residues 16, 18, 21, and 22) or positive (residues 34, 42, 43, and 47). This is mainly due to imprecision in the measurement of very small NOE values.

Clearly, the dynamics of a random coil are complex. We therefore proceeded to fit the ^{15}N relaxation data using two different approaches based on the general model free analysis of Lipari and Szabo (1982). In the first instance (Model 1), the complete data at 500 and 600 MHz for each residue was fit simultaneously using the Lipari and Szabo (1982) spectral density function:

$$J(\omega) = \boldsymbol{S}^2\tau_r/(1 + \omega^2\tau_r^2) + (1 - \boldsymbol{S}^2)\tau_e/(1 + \omega^2\tau_e^2), \quad (1)$$

optimizing the value of the order parameter $\boldsymbol{S}^2$ and the two correlation times, τ_r and τ_e, for each residue independently. This provides an adequate fit to the data within experimental error, and the values of $\boldsymbol{S}^2$, τ_r, and τ_e are summarized in Figure 8A. In the second instance (Model 2), the complete data at 500 and 600 MHz for all residues was fit simultaneously using the extended spectral density function of Clore et al. (1990b)

$$J(\omega) = S_f^2S_s^2\tau_r/(1 + \omega^2\tau_r^2) + (1 - S_f^2)\tau_{e1}/(1 + \omega^2\tau_{e1}^2) + S_f^2(1 - S_s^2)\tau_{e2}/(1 + \omega^2\tau_{e2}^2), \quad (2)$$

optimizing a single global value of the three correlation times τ_r, τ_{e1}, and τ_{e2}, and the values of the order parameters S_f^2 and S_s^2 for each residue (note that the overall order parameter $\boldsymbol{S}^2 = S_f^2 \cdot S_s^2$). In addition, in the case of the fit using Equation 2, it was necessary to introduce an exchange line-broadening term Δex given by

$$1/T_2(\text{obs}) = 1/T_2 + \pi\Delta\text{ex}, \quad (3)$$

[with $\pi\Delta\text{ex}(500) = \pi\Delta\text{ex}(600) \times 0.694$] for a small number of residues (namely, residues 22 and 23, 27–32, and 44–51). The fit to the experimental data for the spectral density function given by Equation 2 is shown in Figure 7 and is of the same quality as that obtained using Model 1. Plots of the optimized values of $\boldsymbol{S}^2$, S_f^2, and S_s^2 as a function of residue number are shown in Figure 8B.

The values of the overall order parameters $\boldsymbol{S}^2$ are fairly uniform across residues 6–52, with average values of 0.49 ± 0.04 and 0.46 ± 0.03 for Models 1 and 2, respectively. Moreover, the RMS difference between the values of $\boldsymbol{S}^2$ on a residue by residue basis derived using Models 1 and 2 is extremely small (0.046), indicating that the values obtained for $\boldsymbol{S}^2$ are essentially independent of which of the two models is used (Fig. 8). These values are a factor of about 1.6–1.7 smaller than the values of $\boldsymbol{S}^2$ typically observed for the cores of folded proteins (Kay et al., 1989; Clore et al., 1990a; Kördel et al., 1992; Redfield et al., 1992; Barchi et al., 1994), but are comparable to those observed in flexible linker or loop regions (Clore et al., 1990a; Barbato et al., 1992; Akke et al., 1993). Interestingly, $\boldsymbol{S}^2$ varies over a very small range, 0.4–0.5, over residues 6–52. This is in stark contrast to the results obtained for a disordered 131-residue fragment of staphylococcal nuclease (Alexandrescu & Shortle, 1994) and for a few selected residues of an unfolded SH3 domain in equilibrium with the folded state under aqueous conditions (Farrow et al., 1995). In these two latter cases,

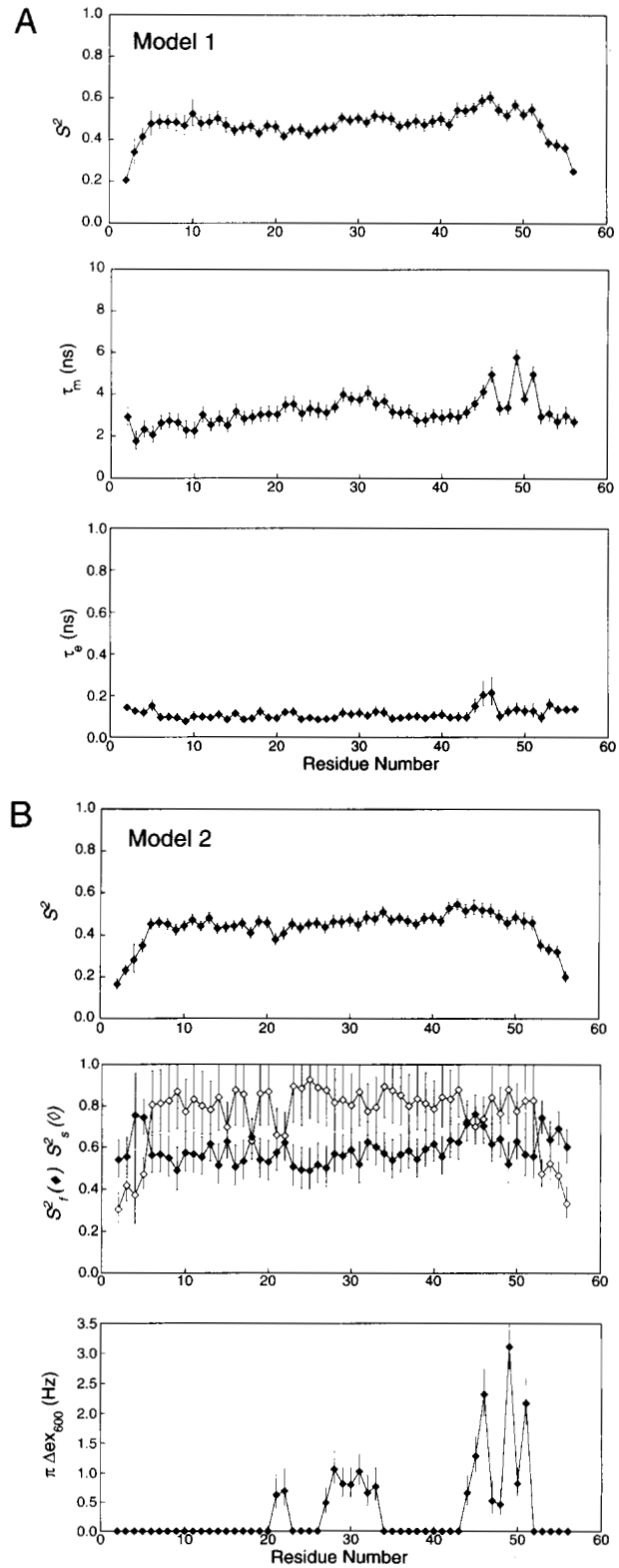

Fig. 8. Variation as a function of residue in the various parameters describing Models 1 ($\boldsymbol{S}^2$, τ_m and τ_e) and 2 ($\boldsymbol{S}^2$, S_f^2, S_s^2, $\pi\Delta$ex) obtained from a nonlinear least-squares best fit of the data shown in Figure 7 to Equations 1 and 2, respectively. Standard deviations in the fitted parameters are shown as vertical bars. In the case of Model 2, single global values of the correlation times τ_m, τ_{e1}, and τ_{e2} are used to fit the data, the exchange term ($\pi\Delta$ex) was only required for residues 21–22, 27–33, and 44–51, and $\boldsymbol{S}^2 = S_f^2 \cdot S_s^2$.

S^2 varies from 0.05 to 0.8 and from 0.2 to 0.8, respectively, excluding residues at the N- and C-termini. At the N- and C-termini of unfolded GB1, however, there is a significant decrease in the values of S^2, which drop to about 0.1 for residues 2 and 56. These results suggest that unfolded GB1 forms a somewhat compact random coil with uniform dynamic properties on the subnanosecond time scale except for three to four residues at the N- and C-termini, where the amplitude of the subnanosecond motions are significantly increased as a result of end effects.

In the case of Model 2, S^2 is the product of two order parameters S_f^2 and S_s^2. S_f^2 is relatively uniform throughout the sequence with an average value of 0.59 ± 0.07. S_s^2, on the other hand, displays large decreases at the N- and C-termini, and hence contributes to the decrease in S^2 for these residues. The average value of S_s^2 for residues 6–52 is 0.81 ± 0.07. Thus, in Model 2, the faster motion associated with τ_{e1} is of significantly larger amplitude than the smaller one associated with τ_{e2}.

In Model 1, values of τ_m and τ_e are obtained independently for each residue. The average values of τ_m and τ_e are 3.19 ± 0.69 ns and 112 ± 3 ps, respectively. In the case of Model 2, single global values of τ_m, τ_{e1}, and τ_{e2} are used to fit the relaxation data for all the residues simultaneously and these have values of 2.92 ± 0.06 ns, 75 ± 20 ps, and 400 ± 80 ps, respectively. Thus, the overall correlation times τ_m obtained by the two methods of analysis are in good agreement. It is interesting to note that the overall rotational correlation time of folded GB1 at 25 °C is 3.3 ± 0.02 ns (Barchi et al., 1994). To compare the values of τ_m for the folded and unfolded states of GB1, it is essential to take into account the viscosity of the solutions, because τ_m scales linearly with viscosity. Because the viscosity of a solution of 7.4 M urea is 1.56-fold higher than that of water (Weast & Astle, 1983), we conclude that, at the same solution viscosity, the apparent overall tumbling rate of unfolded GB1 is a factor of about 1.7 times higher than that for the folded state.

As noted above, the T_1 and T_2 values are significantly reduced for residues 42–51, and the T_2 values are also reduced for residues 21–22 and 28–33 (Fig. 7). In the case of Model 1, this is accommodated by corresponding increases in the values of τ_m, and, in the case of residues 44–46, by τ_e as well (Fig. 8A). In the case of Model 2, on the other hand, the T_2 effects are manifested by the necessity to include a chemical exchange term, which again essentially mirrors the T_2 variation in these three regions (Fig. 8B). Although an exact physical model of this phenomenon is not feasible, owing to the fact that unfolded GB1 is not a globular protein, these results clearly indicate that some sort of conformationally restrictive motion must be taking place in these regions, either on the nanosecond time scale in the case of Model 1, or a time scale of ~4 μs to about 2 ms in the case of Model 2 (Powers et al., 1992). (Note that for Model 2, the lower limit of the lifetime τ_{ex} of the exchange process is given by $\tau_{ex} \sim 2\Delta ex/[\pi(\nu_A - \nu_B)^2]$, where ν_A and ν_B are the chemical shifts of states A and B, respectively, assuming a maximum ^{15}N chemical shift difference of 2 ppm and a minimum detectable increase in line width Δex of 0.1 Hz; the upper limit is determined by the 400-μs time interval between the refocusing pulses of the Carr–Purcell–Meinboom–Gill sequence used to measure T_2). It is interesting to note that the three regions correspond to the N-terminus and middle of the single α-helix and to the second β-hairpin (between strands 3 and 4) in folded GB1 (Fig. 1). The dynamic data may therefore be interpreted to be suggestive of the presence of some transient medium- or long-range structure in these three regions whose population and lifetime are sufficiently small and short, respectively, that no nonsequential ^1H-^1H NOEs can be observed.

Concluding remarks

In contrast to other denatured proteins that have been studied by NMR (Neri et al., 1992a, 1992b, 1992c; Logan et al., 1993, 1994; Shortle & Abeygunawardana, 1993; Stockman et al., 1993; Arcus et al., 1994; Alexandrescu et al., 1994; Alexandrescu & Shortle, 1994), the chemical shift, ^1H-^1H NOE and coupling constant data show no evidence for the presence of any residual partially populated structure in the urea-unfolded state of GB1 at pH 2. Thus, the unfolded state of GB1 characterized in this paper probably represents the closest example of a random coil unfolded protein observed to date. The ^{15}N relaxation data, however, provide evidence for conformationally restricted motion in three segments of the unfolded polypeptide corresponding to the second β-hairpin (where the phenomenon is most marked), the middle of the α-helix, and the N-terminus of the α-helix of folded GB1. Because the dynamics of unfolded GB1 are highly complex, it is uncertain whether these motions occur on a time scale that is only a factor of about two slower than the apparent average (per residue) correlation time of ~3 ns (as deduced from the spectral density function given by Equation 1), or whether they give rise to chemical exchange line broadening (as deduced from the spectral density function given by Equation 2), in which case the time scale may range from about 4 μs to 2 ms. Moreover, it is important to note that these motions do not perturb the values of the overall order parameters S^2, which are only dependent on internal motions occurring on the subnanosecond time scale and are fairly uniform, varying over a range from 0.4 to 0.5 (for residues 6–52), except at the N- and C-termini, where end effects predominate. Irrespective of the interpretation, the population of ordered structure in these three regions is too small to permit the observation of ^1H-^1H NOEs. It is possible that these three regions may comprise potential nucleation sites for folding. In this regard, three observations are of interest. First, the three regions correspond to the segments of the polypeptide that show apparent protection factors for ND-NH exchange up to 10-fold higher than that expected for a random coil in the apparent initial state observed in the folding of GB1 by quenched flow D-H exchange (Kuszewski et al., 1994). Second, a 16-residue peptide comprising the second β-hairpin has been shown by NMR to contain a population of about 40% native-like β-hairpin structure in pure water (Blanco et al., 1994b). Third, a 20-residue peptide corresponding to the α-helix of GB1 has been shown to easily adopt an α-helical conformation upon addition of only small amounts of trifluoroethanol (Blanco & Serrano, 1995).

Materials and methods

Sample preparation

GB1 was expressed and purified as described previously (Gronenborn et al., 1991; Gronenborn & Clore, 1993). Uniformly (>95%) ^{15}N- and $^{15}N/^{13}C$-labeled GB1 domain was prepared by growing the bacteria on minimal medium using $^{15}NH_4Cl$ and $^{13}C_6$-glucose as the sole nitrogen and carbon sources, respectively. The samples

for NMR contained approximately 0.5 mM protein, 7.4 M urea, pH 2.0.

NMR spectroscopy

All experiments were carried out at 25 °C on a Bruker AMX600 spectrometer equipped with a triple resonance z-shielded gradient probe. With the exception of the 3D HBHA(CBCA)NH (Wang et al., 1994) and ^{13}C-^{13}C-^{1}H AMNESIA (Grzesiek & Bax, 1995) experiments, details of the multidimensional heteronuclear NMR experiments used for through-bond sequential assignment, and the observation of ^{1}H-^{1}H NOEs, together with the original references, are provided in the following reviews: Bax and Grzesiek (1993); Clore and Gronenborn (1991, 1994). Three-bond $^{3}J_{HN\alpha}$ coupling constants were obtained by quantitative J correlation spectroscopy (Vuister & Bax, 1993; Bax et al., 1994).

^{15}N relaxation measurements were performed at 500 and 600 MHz as described previously (Kay et al., 1992; Barchi et al., 1994). Heteronuclear ^{1}H-^{15}N NOE measurements used the water flip-back method to avoid saturation of the amide resonances (Grzesiek & Bax, 1993). Solvent signal suppression was obtained by application of a WATERGATE sequence (Piotto et al., 1992), and all experiments employed pulsed field gradients for artifact suppression (Bax & Pochapsky, 1992). Ten T delays were used for T_1 (48, 96, 256, 384, 512, 656, 832, 1,024, 1,136, and 1,328 ms) and T_2 (16, 32, 64, 96, 128, 160, 256, 304, 400, and 640 ms). The recycle time was 1.2 s for the ^{15}N T_1 and T_2 experiments and 3 s for the NOE experiments. The decays of cross-peaks intensities with time in the ^{15}N T_1 and T_2 experiments were fit to a single exponential by nonlinear least-squares methods. Fitting errors of the T_1 and T_2 values were typically less than 2%. Errors in the NOE measurements were of the order of ±0.1–0.15. Model free parameters were determined by nonlinear least-squares Powell minimization of the sum of the error-weighted residuals between the calculated and experimental data using the program FACSIMILE (Chance et al., 1979). Errors in the fitted parameters were obtained from a conventional analysis of the variance-covariance matrix generated by the nonlinear least-squares optimization routine.

Acknowledgments

We thank Attila Szabo and John Kuszewski for many helpful and stimulating discussions, Dan Garrett and Frank Delaglio for software support, and Rolf Tschudin for hardware support. This work was supported by the AIDS Targeted Antiviral Program of the Office of the Director of the National Institutes of Health (to G.M.C. and A.M.G.).

References

Achari A, Hale SP, Howard AJ, Clore GM, Gronenborn AM, Hardman KD, Whitlow M. 1992. 1.67-Å X-ray structure of the B2 immunoglobulin-binding domain of streptococcal protein G and comparison to the NMR structure of the B1 domain. *Biochemistry 31*:10449–10457.

Akke M, Skelton NJ, Kördel J, Palmer AG, Chazin WJ. 1993. Effects of ion binding on the backbone dynamics of calbinin D_{9k} determined by ^{15}N NMR relaxation. *Biochemistry 32*:9832–9844.

Alexander P, Orban J, Bryan P. 1992. Kinetic analysis of folding and unfolding of the 56 amino acid IgG-binding domain of streptococcal protein G. *Biochemistry 31*:7243–7248.

Alexandrescu AT, Abeygunawardana C, Shortle D. 1994. Structure and dynamics of a denatured 131-residue fragment of staphylococcal nuclease: A heteronuclear NMR study. *Biochemistry 33*:1063–1072.

Alexandrescu AT, Evans PA, Pitkeathly M, Baum J, Dobson CM. 1993. Structure and dynamics of the acid-denatured molten globule state of alpha-lactalbumin: A two-dimensional NMR study. *Biochemistry 32*: 1707–1718.

Alexandrescu AT, Shortle D. 1994. Backbone dynamics of a highly disordered 131 residue fragment of staphylococcal nuclease. *J Mol Biol 242*: 527–546.

Barchi JJ, Grasberger B, Gronenborn AM, Clore GM. 1994. Investigation of the backbone dynamics of the IgG-binding domain of streptococcal protein G by heteronuclear two-dimensional ^{1}H-^{15}N nuclear magnetic resonance spectroscopy. *Protein Sci 3*:15–21.

Bax A, Grzesiek S. 1993. Methodological advances in protein NMR. *Acc Chem Res 26*:131–138.

Bax A, Pochapsky S. 1992. Optimized recording of heteronuclear multidimensional NMR spectra using pulse field gradients. *J Magn Reson 99*:638–643.

Bax A, Vuister GW, Grzesiek S, DeLaglio F, Wang AC, Tschudin R, Zhu G. 1994. Measurement of homo- and heteronuclear J couplings from quantitative J correlation. *Methods Enzymol 239*:79–105.

Blanco FJ, Jiménez MA, Pineda A, Rico M, Santoro J, Nieto JL. 1994a. NMR solution structure of the isolated N-terminal fragment of protein-G B1 domain. Evidence of trifluoroethanol induced native-like β-hairpin formation. *Biochemistry 33*:6004–6014.

Blanco FJ, Rivas G, Serrano L. 1994b. A short linear peptide that folds into a native stable β-hairpin in aqueous solution. *Nature Struct Biol 1*:584–589.

Blanco FJ, Serrano L. 1995. Folding of protein G B_1 domain studied by conformational characterization of fragments comprising its secondary structure elements. *Eur J Biochem 230*:634–649.

Bundi A, Wüthrich K. 1979. ^{1}H-NMR parameters of the common amino acid residues measured in aqueous solutions of the linear tetrapeptides H-Gly-Gly-X-L-Ala-OH. *Biopolymers 18*:285–297.

Chance EM, Curtis AR, Jones IP, Kirby CR. 1979. FACSIMILE: A computer program for flow and chemistry simulation and general initial value problems. *UK Atomic Energy Authority, Harwell (Rep.) RE-R8775.*

Clore GM, Driscoll PC, Wingfield PT, Gronenborn AM. 1990a. Analysis of the backbone dynamics of interleukin-1β using two-dimensional inverse detected heteronuclear ^{15}N-^{1}H NMR spectroscopy. *Biochemistry 29*:7387–7401.

Clore GM, Gronenborn AM. 1991. Structures of larger proteins in solution: Three- and four-dimensional heteronuclear NMR spectroscopy. *Science 252*:1390–1399.

Clore GM, Gronenborn AM. 1994. Multidimensional heteronuclear magnetic resonance of proteins. *Methods Enzymol 239*:349–363.

Clore GM, Szabo A, Bax A, Kay LE, Driscoll PC, Gronenborn AM. 1990b. Deviations from the simple two-parameter model-free approach to the interpretation of nitrogen-15 nuclear magnetic relaxation of proteins. *J Am Chem Soc 112*:4989–4991.

Dobson CM. 1992. Unfolded proteins, compact states and molten globules. *Curr Opin Struct Biol 2*:6–12.

Farrow NA, Zhang O, Forman-Kay JD, Kay LE. 1995. Comparison of the backbone dynamics of a folded and an unfolded SH3 domain existing in equilibrium in aqueous buffer. *Biochemistry 34*:868–878.

Gallagher T, Alexander P, Bryan P, Gilliland GL. 1994. Two crystal structures of the B1 immunoglobin-binding domain of streptococcal protein G and comparison with NMR. *Biochemistry 33*:4721–4729.

Gronenborn AM, Clore GM. 1993. Identification of the contact surface of a streptococcal protein G domain complexed with a human Fc fragment. *J Mol Biol 233*:331–335.

Gronenborn AM, Filpula DR, Essig NZ, Achari A, Whitlow M, Wingfield PT, Clore GM. 1991. A novel, highly stable fold of the immunoglobulin binding domain of streptococcal protein G. *Science 253*:657–661.

Grzesiek S, Bax A. 1993. The importance of not saturating H_2O in protein NMR: Application to sensitivity enhancement and NOE measurements. *J Am Chem Soc 115*:12593–12595.

Grzesiek S, Bax A. 1995. Audio-frequency NMR in a mutating frame: Application to the assignment of phenylalanine residues in isotopically enriched proteins. *J Am Chem Soc 117*:6527–6531.

Ikura M, Kay LE, Bax A. 1990. Three-dimensional NOESY-HMQC spectroscopy of a ^{13}C-labeled protein. *J Magn Reson 86*:204–209.

Kay LE, Nicholson LK, Delaglio F, Bax A, Torchia DA. 1992. Backbone dynamics of proteins as studied by ^{15}N inverse detected heteronuclear NMR spectroscopy: Application to staphylococcal nuclease. *J Magn Reson 97*:359–375.

Kay LE, Torchia DA, Bax A. 1989. Backbone dynamics of proteins as stud-

ied by ^{15}N inverse detected heteronuclear NMR spectroscopy: Application to staphylococcal nuclease. *Biochemistry 28*:8972–8979.
Kördel J, Skelton NJ, Akke M, Palmer AG, Chazin WJ. 1992. Backbone dynamics of calcium loaded calbindin D_{9k} studied by two-dimensional proton detected ^{15}N NMR spectroscopy. *Biochemistry 31*:4856–4866.
Kraulis PJ. 1991. MOLSCRIPT: A program to produce both detailed and schematic plots of protein structures. *J Appl Crystallogr 24*:946–950.
Kuszewski J, Clore GM, Gronenborn AM. 1994. Fast folding of a prototypic polypeptide: The immunoglobulin binding domain of streptococcal protein G. *Protein Sci 3*:1945–1952.
Lipari G, Szabo A. 1982. Model-free approach to the interpretation of nuclear magnetic resonance relaxation in macromolecules. 1. Theory and range of validity. *J Am Chem Soc 104*:4546–4559.
Le H, Oldfield E. 1994. Correlation between ^{15}N NMR chemical shifts in protein and secondary structure. *J Biomol NMR 4*:341–348.
Logan TM, Olejniczak ET, Xu RX, Fesik SW. 1993. A general method for assigning NMR spectra of denatured proteins using 3D HC(CO)NH-TOCSY triple resonance experiments. *J Biomol NMR 3*:225–231.
Logan TM, Thériault Y, Fesik SW. 1994. Structural characterization of the FK506 binding protein unfolded in urea and guanidine hydrochloride. *J Mol Biol 236*:637–648.
Lumb KJ, Kim PS. 1994. Formation of a hydrophobic cluster in denatured bovine pancreatic trypsin inhibitor. *J Mol Biol 236*:412–420.
Marion D, Driscoll PC, Kay LE, Wingfield PT, Bax A, Gronenborn AM, Clore GM. 1989. Overcoming the overlap problem in the assignment of ^{1}H-NMR spectra of larger proteins using three-dimensional heteronuclear ^{1}H-^{15}N Hartmann–Hahn-multiple quantum coherence and nuclear Overhauser-multiple quantum coherence spectroscopy: Application to interleukin-1β. *Biochemistry 28*:6150–6156.
Merutka G, Dyson HJ, Wright PE. 1995. "Random coil" ^{1}H chemical shifts obtained as a function of temperature and trifluoroethanol concentration for the peptide series GGXGG. *J Biomol NMR 5*:14–24.
Neri D, Billeter M, Wider G, Wüthrich K. 1992a. NMR determination of residual structure in a urea-denatured protein, the 434-repressor. *Science 257*:1559–1563.
Neri D, Wider G, Wüthrich K. 1992b. Complete ^{15}N and ^{1}H NMR assignments for the amino-terminal domain of the phage 434 repressor in the urea-unfolded form. *Proc Natl Acad Sci USA 89*:4397–4401.
Neri D, Wider G, Wüthrich K. 1992c. ^{1}H, ^{15}N and ^{13}C NMR assignments of the 434 repressor fragments 1–63 and 44–64 unfolded in 7 M urea. *FEBS Lett 303*:129–135.
Pace CN, Shirley BA, Thomson JA. 1989. Measuring the conformational stability of a protein. In: Creighton TE, ed. *Protein structure—A practical approach*. Oxford, UK: IRL Press. pp 311–330.
Piotto M, Saudek V, Skelnar V. 1992. Gradient-tailored excitation for single quantum NMR spectroscopy of aqueous solutions. *J Biomol NMR 1*:661–665
Powers R, Clore GM, Stahl SJ, Wingfield PT, Gronenborn AM. 1992. Analysis of the backbone dynamics of the ribonuclease H domain of the human immunodeficiency virus reverse transcriptase using ^{15}N relaxation measurements. *Biochemistry 31*:9150–9157.
Redfield C, Boyd J, Smith LJ, Smith RAG, Dobson CM. 1992. Loop mobility in a four-helix bundle protein: ^{15}N NMR relaxation measurements on human interleukin-4. *Biochemistry 31*:10431–10437.
Richarz R, Wüthrich K. 1978. Carbon-13 NMR chemical shifts of the common amino acid residues measured in aqueous solutions of the linear tetrapeptides H-Gly-Gly-X-L-Ala-OH. *Biopolymers 17*:2133–2141.
Shortle D. 1993. Denatured states of proteins and their roles in folding and stability. *Curr Opin Struct Biol 3*:66–74.
Shortle D, Abeygunawardana C. 1993. NMR analysis of the residual structure in the denatured state of an unusual mutant of staphylococcal nuclease. *Structure 1*:121–134.
Spera S, Bax A. 1991. Empirical correlation between protein backbone conformation and Cα and Cβ ^{13}C nuclear magnetic resonance chemical shifts. *J Am Chem Soc 113*:5490–5492.
Stockman BJ, Euvrard A, Scahill TA. 1993. Heteronuclear three-dimensional NMR spectroscopy of a partially denatured protein: The A-state of human ubiquitin. *J Biomol NMR 3*:285–296.
Vuister GW, Bax A. 1993. Quantitative J correlation: A new approach for measuring homonuclear three-bond $J(H^{N}H^{\alpha})$ coupling constants in ^{15}N-enriched proteins. *J Am Chem Soc 115*:7772–7777.
Wang AC, Lodi PJ, Qin J, Vuister GW, Gronenborn AM, Clore GM. 1994. An efficient triple-resonance experiment for proton-directed sequential backbone assignment of medium-sized proteins. *J Magn Reson B 105*: 196–198.
Weast RC, Astle MJ. 1983. *CRC handbook of chemistry and physics*. Boca Raton, Florida: CRC Press.
Wishart DS, Bigam CG, Holm A, Hodges RS, Sykes BD 1995. ^{1}H, ^{13}C and ^{15}N random coil NMR chemical shifts of the common amino acids. I. Investigations of nearest-neighbor effects. *J Biomol NMR 5*:67–81.
Zhang O, Kay LE, Olivier JP, Forman-Kay JD. 1994. Backbone ^{1}H and ^{15}N resonance assignments of the N-terminal SH3 domain of drk in folded and unfolded states using enhanced-sensitivity pulsed field gradient NMR techniques. *J Biomol NMR 4*:845–858.